
Lifelong Policy Gradient Learning of Factored Policies for Faster Training Without Forgetting

Jorge A. Mendez¹, Boyu Wang², and Eric Eaton¹

¹Department of Computer and Information Science
University of Pennsylvania
{mendezme,eeaton}@seas.upenn.edu

²Department of Computer Science
University of Western Ontario
bwang@csd.uwo.ca

Abstract

Policy gradient methods have shown success in learning control policies for high-dimensional dynamical systems. Their biggest downside is the amount of exploration they require before yielding high-performing policies. In a lifelong learning setting, in which an agent is faced with multiple consecutive tasks over its lifetime, reusing information from previously seen tasks can substantially accelerate the learning of new tasks. We provide a novel method for lifelong policy gradient learning that trains lifelong function approximators directly via policy gradients, allowing the agent to benefit from accumulated knowledge throughout the entire training process. We show empirically that our algorithm learns faster and converges to better policies than single-task and lifelong learning baselines, and completely avoids catastrophic forgetting on a variety of challenging domains.

1 Introduction

Policy gradient (PG) methods have been successful in learning control policies on high-dimensional, continuous systems [33, 23, 34]. However, like most methods for reinforcement learning (RL), they require the agent to interact with the world extensively before outputting a functional policy. In some settings, this experience is prohibitively expensive, such as when training an actual physical system.

If an agent is expected to learn multiple consecutive tasks over its lifetime, then we would want it to leverage knowledge from previous tasks to accelerate the learning of new tasks. This is the premise of lifelong RL methods [7, 21]. Most previous work in this field has considered the existence of a central policy that can be used to solve all tasks the agent will encounter. If the tasks are sufficiently related, this model serves as a good starting point for learning new tasks, and the main problem becomes how to avoid forgetting the knowledge required to solve tasks encountered early in the agent’s lifetime.

However, in many cases, the tasks the agent will encounter are less closely related, and so a single policy is insufficient for solving all tasks. A typical approach for handling this (more realistic) setting is to train a separate policy for each new task, and then use information obtained during training to find commonalities to previously seen tasks and use these relations to improve the learned policy. Note that this only enables the agent to improve policy performance *after* an initial policy has been trained. Such methods have been successful in outperforming the original policies trained independently for each task, but unfortunately do not allow the agent to reuse knowledge from previous tasks to more efficiently explore the policy space, and so the learning itself is not accelerated.

We propose a novel framework for lifelong RL via PG learning that automatically leverages prior experience *during* the training process of each task. In order to enable learning highly diverse tasks, we follow prior work in lifelong RL by searching over factored representations of the policy-

parameter space to learn both a shared repository of knowledge and a series of task-specific mappings to constitute individual task policies from the shared knowledge.

Our algorithm, *lifelong PG: faster training without forgetting* (LPG-FTW) yields high-performing policies on a variety of benchmark problems with a surprisingly low amount of experience needed per task, and avoids the problem of *catastrophic forgetting* [24]. Moreover, we show theoretically that LPG-FTW is guaranteed to converge to a particular approximation to the multi-task objective.

2 Related work

A large body of work in lifelong RL is based on parameter sharing, where the underlying relations among multiple tasks are captured by the model parameters. The key problem is designing how to share parameters across tasks in such a way that subsequent tasks benefit from the earlier tasks, and the modification of the parameters by future tasks does not hinder performance of the earlier tasks.

Two broad categories of methods have arisen that differ in the way they share parameters.

The first class of lifelong RL techniques, which we will call single-model, assumes that there is one model that works for all tasks. These algorithms follow some standard single-task learning (STL) PG algorithm, but modify the PG objective to encourage transfer across tasks. A prominent example is elastic weight consolidation (EWC) [21], which imposes a quadratic penalty for deviating from earlier tasks' parameters to avoid forgetting. This idea has been extended by modifying the exact form of the penalty [22, 40, 26, 29, 10, 36], but most of these approaches have not been evaluated in RL. In order for single-model methods to work, they require one of two assumptions to hold: either all tasks must be very similar, or the model must be over-parameterized to capture variations among tasks. The first assumption is clearly quite restrictive, as it would preclude the agent from learning highly varied tasks. The second, we argue, is just as restrictive, since the over-parameterization is finite, and so the model can become saturated after a (typically small) number of tasks.

The second class, which we will call multi-model, assumes that there is a set of shared parameters, representing a collection of models, and a set of task-specific parameters, to select a combination of these models for the current task. A classical example is PG-ELLA [7, 6, 19], which assumes that each task's parameters are factored as a linear combination of dictionary elements. In a first stage, these methods learn a policy for each task in isolation (i.e., ignoring any information from other tasks) to determine similarity to previous policies, and in a second stage, the parameters are factored to improve performance via transfer. The downside of this is that the agent does not benefit from prior experience during initial training, which is critical for efficient learning in a lifelong RL setting.

Our approach, LPG-FTW, uses multiple models like the latter category, but learns these models directly via PG learning like the former class. This enables LPG-FTW to be flexible and handle highly varied tasks while also benefiting from prior information during the learning process, thus accelerating the training. A similar approach has been explored in the context of model-based RL [25], but their focus was discovering when new tasks were encountered in the absence of task indicators.

Other approaches store experiences in memory for future replay [18, 30] or use a separate model for each task [31, 14]. The former is not applicable to PG methods without complex and often unreliable importance sampling techniques, while the latter is infeasible when the number of tasks grows large.

Meta RL [9, 11, 15, 8] and multi-task RL [27, 35, 38, 41] also seek to accelerate learning by reusing information from different tasks, but in those settings the agent does not handle tasks arriving sequentially and the consequent problem of catastrophic forgetting. Instead, there is a large batch of tasks available for training and evaluation is done either on the same batch or on a target task.

3 Problem formulation

In a Markov decision process (MDP) $\langle \mathcal{X}, \mathcal{U}, T, R, \gamma \rangle$, $\mathcal{X} \subseteq \mathbb{R}^d$ is the set of states, $\mathcal{U} \subseteq \mathbb{R}^m$ is the set of actions, $T : \mathcal{X} \times \mathcal{U} \times \mathcal{X} \mapsto [0, 1]$ is the probability $P(\mathbf{x}' | \mathbf{x}, \mathbf{u})$ of going to state \mathbf{x}' after executing action \mathbf{u} in state \mathbf{x} , $R : \mathcal{X} \times \mathcal{U} \mapsto \mathbb{R}$ is the reward function measuring the goodness of a state-action pair, and $\gamma \in [0, 1]$ is the discount factor for future rewards. A policy $\pi : \mathcal{X} \times \mathcal{U} \mapsto [0, 1]$ prescribes the agent's behavior as a probability $P(\mathbf{u} | \mathbf{x})$ of selecting action \mathbf{u} in state \mathbf{x} . The goal of RL is to find the policy π^* that maximizes the expected returns $\mathbb{E} [\sum_{i=0}^{\infty} \gamma^i R_i]$, where $R_i = R(\mathbf{x}_i, \mathbf{u}_i)$.

PG algorithms have shown success in solving continuous RL problems by assuming that the policy π_θ is parameterized by $\theta \in \mathbb{R}^d$ and searching for the set of parameters θ^* that optimizes the long-term rewards: $\mathcal{J}(\theta) = \mathbb{E} [\sum_{i=0}^{\infty} \gamma^i R_i]$ [33, 23, 34]. Different approaches use varied strategies for estimating the gradient $\nabla_\theta \mathcal{J}(\theta)$. However, the common high-level idea is to use the current policy π_θ to sample trajectories of interaction with the environment, and then estimating the gradient as the average of some function of the features and rewards encountered through the trajectories.

We frame lifelong PG learning as online multi-task learning of policy parameters. The agent will face a sequence of tasks $\mathcal{Z}^{(1)}, \dots, \mathcal{Z}^{(T_{\max})}$, each of which will be an MDP $\mathcal{Z}^{(t)} = \langle \mathcal{X}^{(t)}, \mathcal{U}^{(t)}, T^{(t)}, R^{(t)}, \gamma \rangle$. The goal of the agent is to find the set of policy parameters $\{\theta^{(1)}, \dots, \theta^{(T_{\max})}\}$ that maximizes the performance across all tasks: $\frac{1}{T_{\max}} \sum_{t=1}^{T_{\max}} \mathbb{E} \sum_{i=0}^{\infty} \gamma^i R_i^{(t)}$. We do not assume knowledge of the total number of tasks, the order in which tasks will arrive, or the relations between different tasks.

Upon observing each task, the agent will be allowed to interact with the environment for a limited time, typically insufficient for obtaining optimal performance without exploiting information from prior tasks. During this time, the learner will strive to discover any relevant information from the current task to 1) relate it to previously stored knowledge in order to permit transfer and 2) store any newly discovered knowledge for future reuse. At any time, the agent may be evaluated on any previously seen task, so it must retain knowledge from all early tasks in order to perform well.

4 Lifelong policy gradient learning

Our framework for lifelong PG learning uses factored representations. The central idea is assuming that the policy parameters for task t can be factored into $\theta^{(t)} \approx \mathbf{L} \mathbf{s}^{(t)}$, where $\mathbf{L} \in \mathbb{R}^{d \times k}$ is a shared dictionary of policy factors and $\mathbf{s}^{(t)} \in \mathbb{R}^k$ are task-specific coefficients that select components for the current task. We further assume that we have access to some base PG algorithm that, given a single task, is capable of finding a parametric policy that performs well on the task, although not necessarily optimally.

Upon encountering a new task t , LPG-FTW (Algorithm 1) will use the base learner to optimize the task-specific coefficients $\mathbf{s}^{(t)}$, without modifying the knowledge base \mathbf{L} . This corresponds to searching for the optimal policy that can be obtained by combining the factors of \mathbf{L} . Every $M \gg 1$ steps, the agent will update the knowledge base \mathbf{L} with any relevant information collected from t up to that point. This allows the agent to search for policies with an improved knowledge base in subsequent steps.

Concretely, the agent will strive to solve the following optimization during the training phase:

$$\mathbf{s}^{(t)} = \arg \max_{\mathbf{s}} \ell(\mathbf{L}_{t-1}, \mathbf{s}) = \arg \max_{\mathbf{s}} \mathcal{J}^{(t)}(\mathbf{L}_{t-1} \mathbf{s}) - \mu \|\mathbf{s}\|_1, \quad (1)$$

where $\mathcal{J}^{(t)}(\cdot)$ is any PG objective and the ℓ_1 norm encourages sparsity. The agent will then optimize the second-order approximate multi-task objective to incorporate new knowledge into the dictionary:

$$\mathbf{L}_t = \arg \max_{\mathbf{L}} \hat{g}_t(\mathbf{L}) = \arg \max_{\mathbf{L}} -\lambda \|\mathbf{L}\|_F^2 + \frac{1}{t} \sum_{\hat{t}=1}^t \hat{\ell}(\mathbf{L}, \mathbf{s}^{(\hat{t})}, \boldsymbol{\alpha}^{(\hat{t})}, \mathbf{H}^{(\hat{t})}, \mathbf{g}^{(\hat{t})}), \quad (2)$$

where $\mathbf{g}^{(\hat{t})} = \nabla_{\theta} \mathcal{J}^{(\hat{t})}(\theta)|_{\theta=\boldsymbol{\alpha}^{(\hat{t})}}$ and $\mathbf{H}^{(\hat{t})} = \frac{1}{2} \nabla_{\theta, \theta^\top} \mathcal{J}^{(\hat{t})}(\theta)|_{\theta=\boldsymbol{\alpha}^{(\hat{t})}}$ are the gradient and Hessian of $\mathcal{J}^{(\hat{t})}(\theta)$ evaluated at $\boldsymbol{\alpha}^{(\hat{t})} = \mathbf{L}_{\hat{t}-1} \mathbf{s}^{(\hat{t})}$ and $\hat{\ell}(\mathbf{L}, \mathbf{s}, \boldsymbol{\alpha}, \mathbf{H}, \mathbf{g}) = -\mu \|\mathbf{s}\|_1 + \|\boldsymbol{\alpha} - \mathbf{L} \mathbf{s}\|_{\mathbf{H}}^2 + \mathbf{g}^\top (\mathbf{L} \mathbf{s} - \boldsymbol{\alpha})$. Unlike Bou Ammar et al. [7], we do not compute the approximation around a single-task optimum,

Algorithm 1 LPG-FTW(d, k, λ, μ, M)

```

 $T \leftarrow 0, \quad \mathbf{L} \leftarrow \text{initializeL}(d, k)$ 
loop
   $t \leftarrow \text{getTask}()$ 
  if isNewTask( $t$ ) then
     $\mathbf{s}^{(t)} \leftarrow \text{initializeSt}(k)$ 
     $T \leftarrow T + 1$ 
  else
     $\mathbf{A} \leftarrow \mathbf{A} - 2 \left( \mathbf{s}^{(t)} \mathbf{s}^{(t)\top} \right) \otimes \mathbf{H}^{(t)}$ 
     $\mathbf{b} \leftarrow \mathbf{b} - \mathbf{s}^{(t)} \otimes (-\mathbf{g}^{(t)} + 2\mathbf{H}^{(t)} \boldsymbol{\alpha}^{(t)})$ 
  for  $i = 1, \dots, N$  do
     $\mathbb{T} \leftarrow \text{getTrajectories}(\mathbf{L} \mathbf{s}^{(t)})$ 
     $\mathbf{s}^{(t)} \leftarrow \text{PGStep}(\mathbb{T}, \mathbf{L}, \mathbf{s}^{(t)}, \mu)$ 
    if  $i \bmod M == 0$  then
       $\boldsymbol{\alpha}^{(t)} \leftarrow \mathbf{L} \mathbf{s}^{(t)}$ 
       $\mathbf{g}^{(t)}, \mathbf{H}^{(t)} \leftarrow \text{gradAndHess}(\boldsymbol{\alpha}^{(t)})$ 
       $\mathbf{A}_t \leftarrow \mathbf{A} + 2 \left( \mathbf{s}^{(t)} \mathbf{s}^{(t)\top} \right) \otimes \mathbf{H}^{(t)}$ 
       $\mathbf{b}_t \leftarrow \mathbf{b} + \mathbf{s}^{(t)} \otimes (-\mathbf{g}^{(t)} + 2\mathbf{H}^{(t)} \boldsymbol{\alpha}^{(t)})$ 
       $\text{vec}(\mathbf{L}) \leftarrow \left( \frac{1}{T} \mathbf{A}_t - 2\lambda \mathbf{I} \right)^{-1} \left( \frac{1}{T} \mathbf{b}_t \right)$ 
     $\mathbf{A} \leftarrow \mathbf{A}_t, \quad \mathbf{b} \leftarrow \mathbf{b}_t$ 

```

enabling LPG-FTW to update \mathbf{L} without finding the (often infeasible) optimum. The solution to this optimization is $\text{vec}(\mathbf{L}_t) = \mathbf{A}^{-1}\mathbf{b}$, where $\mathbf{A} = -2\lambda\mathbf{I} + \frac{2}{t} \sum_{i=1}^t (\mathbf{s}^{(i)} \mathbf{s}^{(i)\top}) \otimes \mathbf{H}^{(i)}$ and $\mathbf{b} = \frac{1}{t} \sum_{i=1}^t \mathbf{s}^{(i)} \otimes \left(-\mathbf{g}^{(i)} + 2\mathbf{H}^{(i)}\boldsymbol{\alpha}^{(i)} \right)$. Notably, these can be computed incrementally as each new task arrives, so that \mathbf{L} can be updated without preserving data or parameters from earlier tasks.

In Equation 1, the agent leverages knowledge from all previous tasks while training on task t , by searching for $\boldsymbol{\theta}^{(t)}$ in the span of \mathbf{L}_{t-1} . This makes LPG-FTW fundamentally different from prior methods that learn each task’s parameter vector in isolation and subsequently combine prior knowledge to improve performance. One potential drawback is that, by restricting the search to the span of \mathbf{L}_{t-1} , we might miss other, potentially better, policies. However, any set of parameters far from the space spanned by \mathbf{L}_{t-1} would be uninformative for the multi-task objective, since the approximations to the previous tasks would be poor near the current task’s parameters and vice versa.

In Equation 2, LPG-FTW approximates the loss around the current set of parameters $\boldsymbol{\alpha}^{(t)}$ via a second-order expansion and finds the \mathbf{L}_t that optimizes the average approximate cost over all previously seen tasks, ensuring that the agent does not forget the knowledge required to solve them.

Time complexity LPG-FTW introduces an overhead of $O(k \times d)$ per PG step, due to the multiplication of the gradient by \mathbf{L}^\top . Additionally, every $M \gg 1$ steps, the update step of \mathbf{L} takes an additional $O(d^3 k^2)$. If the number of parameters d is too high, we could use faster techniques for solving the inverse of \mathbf{A} in Equation 2, like the conjugate gradient method, or approximate the Hessian with a Kronecker-factored (KFAC) or diagonal matrix. While we didn’t use these approximations, they work well in related methods [7, 29], so we expect LPG-FTW to behave similarly. However, note that the time complexity of LPG-FTW is constant w.r.t. the number of tasks seen, since the cost is computed incrementally. This applies to diagonal matrices, but not to KFAC matrices, which require storing all Hessians and recomputing the cost for every new task, which is infeasible for large numbers of tasks.

4.1 Knowledge base initialization

The intuition we have built holds only when a reasonably good \mathbf{L} matrix has already been learned. But what happens at the beginning of the learning process, when the agent has not yet seen a substantial number of tasks? If we take the naïve approach of initializing \mathbf{L} at random, then the $\mathbf{s}^{(t)}$ ’s are unlikely to be able to find a well-performing policy, and so updates to \mathbf{L} will not leverage any useful information.

One common alternative is to initialize the k columns of \mathbf{L} with the STL solutions to the first k tasks, $\boldsymbol{\alpha}^{(t)}|_{t=1}^k$. This is similar to initializing the k -means cluster centroids with points from the data set [1]. However, when the $\boldsymbol{\alpha}^{(t)}$ ’s are sub-optimal, this method prevents tasks $2-k$ from leveraging information from the earlier tasks, impeding them from achieving potentially higher performance. Moreover, several tasks might rediscover information, leading to wasted resources in terms of both learning and capacity of \mathbf{L} .

We propose an initialization method (Algorithm 2) that enables early tasks to leverage knowledge from previous tasks and prevents the discovery of redundant information. The algorithm starts from an empty dictionary and adds error vectors $\boldsymbol{\epsilon}^{(t)}$ for the initial k tasks. For each task t , we modify the optimization in Equation 1 for learning $\mathbf{s}^{(t)}$ by adding $\boldsymbol{\epsilon}^{(t)}$ as additional learnable parameters, which will find knowledge of task t not contained in \mathbf{L} and then will be incorporated as a column of \mathbf{L} :

$$\mathbf{s}^{(t)}, \boldsymbol{\epsilon}^{(t)} = \arg \max_{\mathbf{s}, \boldsymbol{\epsilon}} \mathcal{J}^{(t)}(\mathbf{L}_{t-1}\mathbf{s} + \boldsymbol{\epsilon}) - \mu\|\mathbf{s}\|_1 - \lambda\|\boldsymbol{\epsilon}\|_2^2.$$

4.2 Base policy gradient algorithms

Now, we show how two STL PG learning algorithms can be used as the base learner of LPG-FTW.

Algorithm 2 InitializeL(d, k, λ, μ)

```

 $T \leftarrow 0, \mathbf{L} \leftarrow \text{empty}(d, 0)$ 
while  $T < k$  do
   $t \leftarrow \text{getTask}()$ 
   $\mathbf{s}^{(t)} \leftarrow \text{initializeSt}(k)$ 
   $T \leftarrow T + 1$ 
  for  $i = 1, \dots, N$  do
     $\mathbb{T} \leftarrow \text{getTrajectories}(\mathbf{L}\mathbf{s}^{(t)})$ 
     $\mathbf{s}^{(t)}, \boldsymbol{\epsilon}^{(t)} \leftarrow \text{PGStep}(\mathbb{T}, \mathbf{L}, \mathbf{s}^{(t)}, \boldsymbol{\epsilon}^{(t)}, \mu)$ 
     $\mathbf{L} \leftarrow \text{addColumn}(\mathbf{L}, \boldsymbol{\epsilon}^{(t)})$ 
     $\boldsymbol{\alpha}^{(t)} \leftarrow \mathbf{L}\mathbf{s}^{(t)} + \boldsymbol{\epsilon}^{(t)}$ 
     $\mathbf{g}^{(t)}, \mathbf{H}^{(t)} \leftarrow \text{gradAndHess}(\boldsymbol{\alpha}^{(t)})$ 
     $\mathbf{A} \leftarrow \mathbf{A} + 2 \left( \mathbf{s}^{(t)} \mathbf{s}^{(t)\top} \right) \otimes \mathbf{H}^{(t)}$ 
     $\mathbf{b} \leftarrow \mathbf{b} + \mathbf{s}^{(t)} \otimes \left( -\mathbf{g}^{(t)} + 2\mathbf{H}^{(t)}\boldsymbol{\alpha}^{(t)} \right)$ 

```

4.2.1 Episodic REINFORCE

Episodic REINFORCE updates parameters as $\theta_j \leftarrow \theta_{j-1} + \eta_j g_{\theta_{j-1}}$, with the policy gradient given by $g_{\theta} = \nabla_{\theta} \mathcal{J}(\theta) = \mathbb{E} [\sum_{i=0}^{\infty} \nabla_{\theta} \log \pi_{\theta}(x_i, u_i) A(x_i, u_i)]$, where $A(x, u)$ is the advantage function.

LPG-FTW would then update the $s^{(t)}$'s as $s_j^{(t)} \leftarrow s_{j-1}^{(t)} + \eta_j \nabla_s [\mathcal{J}^{(t)}(L_{t-1}s) - \mu \|s\|_1] \big|_{s=s_j^{(t)}}$, with the gradient given by $\nabla_s [\mathcal{J}^{(t)}(L_{t-1}s) - \mu \|s\|_1] = L_{t-1}^{\top} g_{L_{t-1}s} - \mu \text{sign}(s)$. The Hessian for Equation 2 is given by $H = \frac{1}{2} \mathbb{E} [\sum_{i=0}^{\infty} \nabla_{\theta, \theta^{\top}} \log \pi_{\theta}(x_i, u_i) A(x_i, u_i)]$, which evaluates to $H = -\frac{1}{2\sigma^2} \mathbb{E} [\sum_{i=0}^{\infty} x x^{\top} A(x_i, u_i)]$ in the case where the policy is a linear Gaussian (i.e., $\pi_{\theta} = \mathcal{N}(\theta^{\top} x, \sigma)$). One major drawback of this is that the Hessian is not negative definite, so Equation 2 might move the policy arbitrarily far from the original policy used for sampling trajectories.

4.2.2 Natural Policy Gradient

The natural PG (NPG) algorithm allows us to get around this issue. We use the formulation followed by Rajeswaran et al. [28], which at each iteration optimizes $\max_{\theta} g_{\theta_{j-1}}^{\top} (\theta - \theta_{j-1})$ subject to the quadratic constraint $\|\theta - \theta_{j-1}\|_{F_{\theta_{j-1}}}^2 \leq \delta$, where $F_{\theta} = \mathbb{E} [\nabla_{\theta} \log \pi_{\theta}(x, u) \nabla_{\theta} \log \pi_{\theta}(x, u)^{\top}]$ is the approximate Fisher information of π_{θ} [20]. The base learner would then update the policy parameters at each iteration as $\theta_j \leftarrow \theta_{j-1} + \eta_{\theta} F_{\theta_{j-1}}^{-1} g_{\theta_{j-1}}$, with $\eta_{\theta} = \sqrt{\delta / (g_{\theta_{j-1}}^{\top} F_{\theta_{j-1}}^{-1} g_{\theta_{j-1}})}$.

To incorporate NPG as the base learner in LPG-FTW, at each step we solve $\max_s g_{s_{j-1}^{(t)}}^{\top} (s - s_{j-1}^{(t)})$ subject to $\|s - s_{j-1}^{(t)}\|_{F_{s_{j-1}^{(t)}}}^2 \leq \delta$, which gives us the update: $s_j^{(t)} \leftarrow s_{j-1}^{(t)} + \eta_{s^{(t)}} F_{s_{j-1}^{(t)}}^{-1} g_{s_{j-1}^{(t)}}$. We compute the Hessian for Equation 2 as $H = -\frac{1}{\eta_{\theta}} F_{\theta_{j-1}}$ by using the equivalent soft-constrained problem: $\hat{\mathcal{J}}(\theta) = g_{\theta_{j-1}}^{\top} (\theta - \theta_{j-1}) + \frac{\|\theta - \theta_{j-1}\|_{F_{\theta_{j-1}}}^2 - \delta}{2\eta_{\theta}}$. This Hessian is negative definite, and thus encourages the parameters to stay close to the original ones, where the approximation is valid.

4.3 Theoretical guarantees

We now show that LPG-FTW converges to the optimal multi-task objective for any ordering over tasks, despite the online approximation of keeping the $s^{(t)}$'s fixed after initial training. We substantially adapt the proofs by Ruvo and Eaton [32] to handle the non-optimality of the $\alpha^{(t)}$'s and the fact that the $s^{(t)}$'s and L optimize different objectives. Complete proofs are available in Appendix A.

The objective defined in Equation 2, \hat{g} , considers the optimization of each $s^{(t)}$ separately with the L_t known up to that point, and is a surrogate for our actual objective:

$$g_t(L) = \frac{1}{t} \sum_{\hat{t}=1}^t \max_{s^{(\hat{t})}} \left\{ \|\alpha^{(\hat{t})} - L s^{(\hat{t})}\|_{H^{(\hat{t})}}^2 + g^{(\hat{t})\top} (L s^{(\hat{t})} - \alpha^{(\hat{t})}) - \mu \|s^{(\hat{t})}\|_1 \right\} - \lambda \|L\|_F^2,$$

which considers the simultaneous optimization of all $s^{(t)}$'s. We define the expected objective as:

$$g(L) = \mathbb{E}_{H^{(t)}, g^{(t)}, \alpha^{(t)}} \left[\max_s \hat{\ell}(L, s, \alpha^{(t)}, H^{(t)}, g^{(t)}) \right],$$

which represents how well a particular L can represent a randomly selected task without modifications.

We show that 1) L_t becomes increasingly stable, 2) \hat{g}_t, g_t , and g converge to the same value, and 3) L_t converges to a stationary point of g . These results are based on the following assumptions:

- The tuples $(H^{(t)}, g^{(t)})$ are drawn *i.i.d.* from a distribution with compact support.
- The sequence $\{\alpha^{(t)}\}_{t=1}^{\infty}$ is stationary and ϕ -mixing.
- The magnitude of $\mathcal{J}^{(t)}(\mathbf{0})$ is bounded by B .
- For all $L, H^{(t)}, g^{(t)}$, and $\alpha^{(t)}$, the largest eigenvalue (smallest in magnitude) of $L_{\gamma}^{\top} H^{(t)} L_{\gamma}$ is at most $-\kappa$, with $\kappa > 0$, where γ is the set of non-zero indices of $s^{(t)} = \arg \max_s \hat{\ell}(L, s, H^{(t)}, g^{(t)}, \alpha^{(t)})$. The non-zero elements of the unique maximizing $s^{(t)}$ are given by: $s_{\gamma}^{(t)} = (L_{\gamma}^{\top} H^{(t)} L_{\gamma})^{-1} (L^{\top} (H^{(t)} \alpha^{(t)} - g^{(t)}) - \mu \text{sign}(s_{\gamma}^{(t)}))$.

Proposition 1. $\mathbf{L}_t - \mathbf{L}_{t-1} = O(\frac{1}{t})$.

Proof sketch. First, we show that the entries of \mathbf{L} , $\mathbf{s}^{(t)}$, and $\boldsymbol{\alpha}^{(t)}$ are bounded by Assumptions A and C and the regularization terms. Next, we show that $\hat{g}_t - \hat{g}_{t-1}$ is $O(\frac{1}{t})$ -Lipschitz. We finish the proof with the facts that \mathbf{L}_{t-1} maximizes \hat{g}_{t-1} and the eigenvalues of the Hessian of \hat{g}_{t-1} are bounded. ■

The critical step for adapting the proof from Ruvolo and Eaton [32] to our algorithm is to introduce the following lemma, which shows the equality of the maximizers of ℓ and $\hat{\ell}$.

Lemma 1. $\hat{\ell}(\mathbf{L}_t, \mathbf{s}^{(t+1)}, \boldsymbol{\alpha}^{(t+1)}, \mathbf{H}^{(t+1)}, \mathbf{g}^{(t+1)}) = \max_{\mathbf{s}} \hat{\ell}(\mathbf{L}_t, \mathbf{s}, \boldsymbol{\alpha}^{(t+1)}, \mathbf{H}^{(t+1)}, \mathbf{g}^{(t+1)})$.

Proof sketch. The fact that the single-task objective $\hat{\ell}$ is a second-order approximation at $\mathbf{s}^{(t+1)}$ of ℓ , along with the fact that $\mathbf{s}^{(t+1)}$ is a maximizer of ℓ , implies that $\mathbf{s}^{(t+1)}$ is also a maximizer of $\hat{\ell}$. ■

Proposition 2. 1. $\hat{g}_t(\mathbf{L}_t)$ converges a.s. 3. $g_t(\mathbf{L}_t) - \hat{g}_t(\mathbf{L}_t)$ converges a.s. to 0
2. $g_t(\mathbf{L}_t) - \hat{g}_t(\mathbf{L}_t)$ converges a.s. to 0 4. $g(\mathbf{L}_t)$ converges a.s.

Proof sketch. First, using Lemma 1, we show that the sum of negative variations of the stochastic process $u_t = \hat{g}_t(\mathbf{L}_t)$ are bounded. Given this result, we show that u_t is a quasi-martingale that converges almost surely (Part 1). This fact, along with a simple lemma of positive sequences, allows us to prove Part 2. The final two parts can be shown due to the equivalence of g and g_t as $t \rightarrow \infty$. ■

Proposition 3. The distance between \mathbf{L}_t and the set of all stationary points of g converges a.s. to 0.

Proof sketch. We use the fact that \hat{g}_t and g have Lipschitz gradients with constants independent of t . This fact, combined with the fact that \hat{g}_t and g converge almost surely completes the proof. ■

5 Experimental evaluation

We evaluated our method on a range of complex continuous control domains, showing a substantial increase in learning speed and a dramatic reduction in catastrophic forgetting. See Appendix B for additional details. Code and training videos are available at github.com/GRASP-ML/LPG-FTW.

Baselines We compared against STL, which does not transfer knowledge across tasks, using NPG as described in Section 4.2.2. We then chose EWC [21] from the single-model family, which places a quadratic penalty for deviating from earlier tasks’ parameters. Finally, we compared against PG-ELLA [7], which factorizes the policy parameters like LPG-FTW, but first uses STL to search for the policy parameters of each task and subsequently factorizes the learned parameters, limiting PG-ELLA’s speed to that of STL. All lifelong algorithms used NPG as the base learning method.

Evaluation procedure We chose the hyper-parameters of NPG to maximize the performance of STL on a single task, and used those hyper-parameters for all agents. For EWC, we searched for the regularization parameter over five tasks on each domain. For LPG-FTW and PG-ELLA, we fixed all regularization parameters to 10^{-5} and the number of columns in \mathbf{L} to $k=5$, unless otherwise noted. In LPG-FTW, we used the simplest setting for the update schedule of \mathbf{L} , $M=N$. All experiments were repeated over five trials with different random seeds for parameter initialization and task ordering.

5.1 Empirical evaluation on OpenAI Gym MuJoCo domains

We first evaluated LPG-FTW on simple MuJoCo environments from OpenAI Gym. We selected the HalfCheetah, Hopper, and Walker-2D environments, and created two different evaluation domains for each: a *gravity* domain, where each task corresponded to a random gravity value between $0.5g$ and $1.5g$, and a *body-parts* domain, where the size and mass of each of four parts of the body (head, torso, thigh, and leg) was randomly set to a value between $0.5\times$ and $1.5\times$ its nominal value. These choices led to highly diverse tasks, as we show in Appendix C. We generated tasks using the gym-extensions [16] package, but modified it so each body part was scaled independently.

We created $T_{\max} = 20$ tasks for HalfCheetah and Hopper domains, and $T_{\max} = 50$ for Walker-2D domains. The agents were allowed to train on each task for a fixed number of iterations before moving on to the next. For these simple experiments, all agents used linear policies. For the Walker-2D *body-parts* domain, we set the capacity of \mathbf{L} to $k = 10$, since we found empirically that it required a higher capacity. The NPG hyper-parameters were tuned without body-parts or gravity modifications.

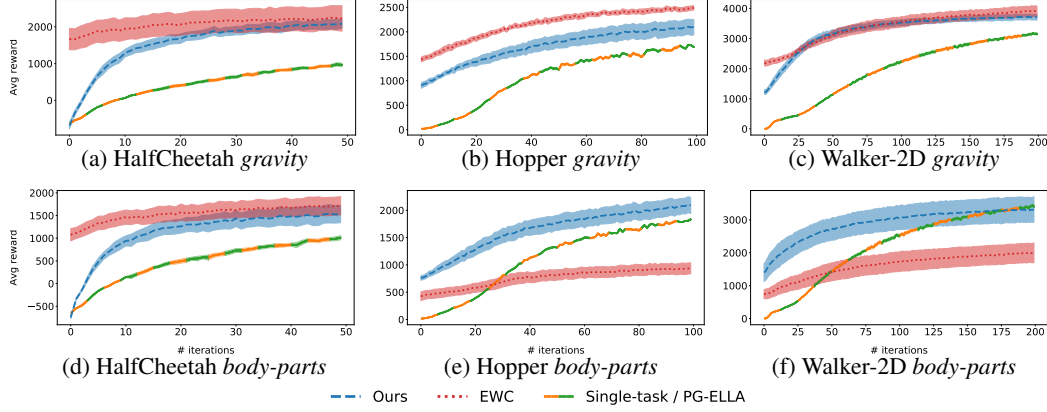


Figure 1: Average performance during training across all tasks for six MuJoCo domains. LPG-FTW is consistently faster than STL and PG-ELLA (which by definition learn at the same pace) in achieving proficiency, and achieves better final performance in five domains and equivalent performance in the remaining one. EWC is faster and converges to higher performance than LPG-FTW in some domains, but completely fails to learn in others. Shaded error bars denote standard error over five random task orderings and parameter initializations.

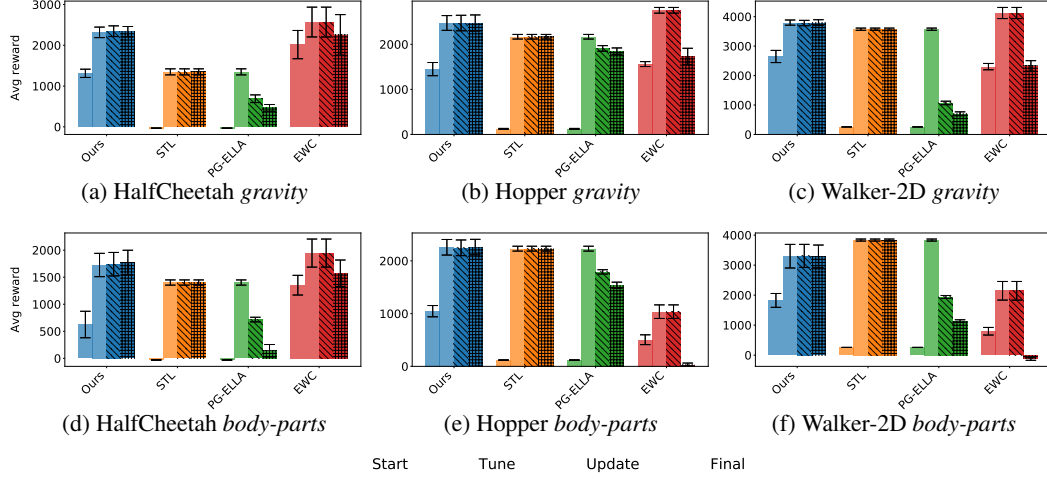


Figure 2: Average performance at the beginning of training (start), after all training iterations (tune), after the update step for PG-ELLA and LPG-FTW (update), and after all tasks have been trained (final). The update step in LPG-FTW never hinders performance, and even after all tasks have been trained performance is maintained. PG-ELLA always performed worse than STL. EWC suffered from catastrophic forgetting in five domains, in two resulting in degradation below initial performance. Error bars denote standard error over five random task orderings and parameter initializations.

Figure 1 shows the average performance over all tasks as a function of the NPG training iterations. LPG-FTW consistently learned faster than STL, and obtained higher final performance on five out of the six domains. Learning the task-specific coefficients $s^{(t)}$ directly via policy search increases the learning speed of LPG-FTW, whereas PG-ELLA is limited to the learning speed of STL, as shown by the shared learning curves. EWC was faster than LPG-FTW in reaching high-performing policies in four domains, primarily due to the fact that the policies are completely shared across tasks, which enables EWC to have starting policies with high performance. However, EWC failed to even match the STL performance in two of the domains. We hypothesize that this is due to the fact that the tasks are highly varied (particularly in the *body-parts* domains, since there are four different axes of variation), and the single shared policy is unable to capture a policy that works in all domains. Appendix D shows an evaluation with various versions of EWC attempting to alleviate these issues.

Results in Figure 1 consider only how fast the agent learns a new task using information from earlier tasks. PG-ELLA and LPG-FTW then perform an update step (Equation 2 for LPG-FTW) where they

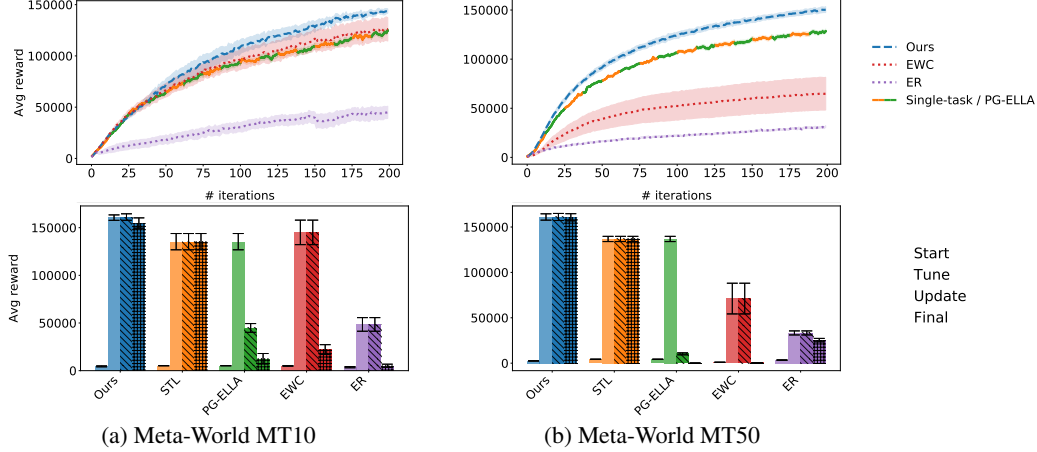


Figure 3: Performance on the Meta-World benchmark. Top: average performance during training across all tasks. Bottom: average performance at the beginning of training (start), after all training iterations (tune), after the update step for PG-ELLA and LPG-FTW (update), and after all tasks have been trained (final). In this notoriously challenging benchmark, LPG-FTW still improves the performance of STL and all baselines, and suffers from no catastrophic forgetting.

incorporate knowledge from the current task into \mathbf{L} . The third bar from the left per each algorithm in Figure 2 shows the average performance after this step, revealing that LPG-FTW maintained performance, whereas PG-ELLA’s performance decreased. This is because LPG-FTW ensures that the approximate objective is computed near points in the parameter space that the current basis \mathbf{L} can generate, by finding $\alpha^{(t)}$ via a search over the span of \mathbf{L} . A critical component of lifelong learning algorithms is their ability to avoid catastrophic forgetting. To evaluate the capacity of LPG-FTW to retain knowledge from earlier tasks, we evaluated the policies obtained from the knowledge base \mathbf{L} trained on all tasks, without modifying the $s^{(t)}$ ’s. The rightmost bar in each algorithm in Figure 2 shows the average final performance across all tasks. LPG-FTW successfully retained knowledge of all tasks, showing no signs of catastrophic forgetting on any of the domains. The PG-ELLA baseline suffered from forgetting in all domains, and EWC in all but one of the domains. Moreover, the final performance of LPG-FTW was the best among all baselines in all but one domain.

5.2 Empirical evaluation on more challenging Meta-World domains

Results so far show that our method improves performance and completely avoids forgetting in simple settings. To showcase the flexibility of our framework, we evaluated it on Meta-World [39], a substantially more challenging benchmark, whose tasks involve using a simulated Sawyer arm to manipulate various objects in diverse ways, and have been shown to be notoriously difficult for state-of-the-art multi-task and meta learning algorithms. We added an experience replay (ER) baseline that uses importance sampling over a replay buffer from all previous tasks’ data to encourage knowledge retention, with a 50-50 replay rate as suggested by Rolnick et al. [30]. We chose the NPG hyper-parameters on the reach task, which is the simplest task from the benchmark. For LPG-FTW and PG-ELLA, we fixed the number of latent components as $k = 3$. All algorithms used a Gaussian policy parameterized by a multi-layer perceptron with two hidden layers of 32 units and tanh activation. Given the high diversity of the tasks considered in this evaluation, we allowed all algorithms to use task-specific output layers, in order to specialize policies to each individual task.

The top row of Figure 3 shows average learning curves across tasks. LPG-FTW again was faster in training, showing that the restriction that the agent only train the $s^{(t)}$ ’s for each new task does not harm its ability to solve complex, highly diverse problems. The difference in learning speed was particularly noticeable in MT50, where single-model methods became saturated. To our knowledge, this is the first time lifelong transfer has been shown on the challenging Meta-World benchmark. The bottom row of Figure 3 shows that LPG-FTW suffered from a small amount of forgetting on MT10. However, on MT50, where \mathbf{L} trained on sufficient tasks for convergence, our method suffered from no forgetting. In contrast, none of the baselines was capable of accelerating the learning, and they all suffered from dramatic forgetting, particularly on MT50, when needing to learn more tasks.

Conclusion

We proposed a method for lifelong PG learning that enables RL learners to quickly learn to solve new tasks by leveraging knowledge accumulated from earlier tasks. We showed empirically that our method, LPG-FTW, does not suffer from catastrophic forgetting, and therefore permits learning a large number of tasks in sequence. Moreover, we prove theoretically that our algorithm is guaranteed to converge to the approximate multi-task objective, despite operating completely online.

Acknowledgments and Disclosure of Funding

The research presented in this paper was partially supported by the Lifelong Learning Machines program from DARPA/MTO under grant #FA8750-18-2-0117.

References

- [1] Anderberg, M. R. (1973). *Cluster Analysis for Applications*. Academic Press, New York, NY.
- [2] Baklanov, E. A. (2006). The strong law of large numbers for L-statistics with dependent data. *Siberian Mathematical Journal*, 47(6):975–979.
- [3] Billingsley, P. (1968). *Convergence of probability measures*. John Wiley & Sons.
- [4] Bonnans, J. F. and Shapiro, A. (1998). Optimization problems with perturbations: A guided tour. *SIAM review*, 40(2):228–264.
- [5] Bottou, L. (2009). On-line learning and stochastic approximations. In Saad, D., editor, *On-line learning in neural networks*, chapter 2, pages 9–42. Cambridge University Press.
- [6] Bou Ammar, H., Eaton, E., Luna, J. M., and Ruvolo, P. (2015). Autonomous cross-domain knowledge transfer in lifelong policy gradient reinforcement learning. In *Proceedings of the Twenty-Fourth International Joint Conference on Artificial Intelligence (IJCAI-15)*, pages 3345–3351.
- [7] Bou Ammar, H., Eaton, E., Ruvolo, P., and Taylor, M. (2014). Online multi-task learning for policy gradient methods. In *Proceedings of the 31st International Conference on Machine Learning (ICML-14)*, pages 1206–1214.
- [8] Clavera, I., Nagabandi, A., Liu, S., Fearing, R. S., Abbeel, P., Levine, S., and Finn, C. (2019). Learning to adapt in dynamic, real-world environments through meta-reinforcement learning. In *7th International Conference on Learning Representations (ICLR-19)*.
- [9] Duan, Y., Schulman, J., Chen, X., Bartlett, P. L., Sutskever, I., and Abbeel, P. (2016). RL^2 : Fast reinforcement learning via slow reinforcement learning. *arXiv preprint arXiv:1611.02779*.
- [10] Ebrahimi, S., Elhoseiny, M., Darrell, T., and Rohrbach, M. (2020). Uncertainty-guided continual learning with Bayesian neural networks. In *8th International Conference on Learning Representations (ICLR-20)*.
- [11] Finn, C., Abbeel, P., and Levine, S. (2017). Model-agnostic meta-learning for fast adaptation of deep networks. In *Proceedings of the 34th International Conference on Machine Learning (ICML-17)*, pages 1126–1135.
- [12] Fisk, D. (1965). Quasi-martingales. *Transactions of the American Mathematical Society*, 120(3):369–389.
- [13] Fuchs, J.-J. (2005). Recovery of exact sparse representations in the presence of bounded noise. *IEEE Transactions on Information Theory*, 51(10):3601–3608.
- [14] Garcia, F. and Thomas, P. S. (2019). A meta-MDP approach to exploration for lifelong reinforcement learning. In *Advances in Neural Information Processing Systems 32 (NeurIPS-19)*, pages 5692–5701.

- [15] Gupta, A., Mendonca, R., Liu, Y., Abbeel, P., and Levine, S. (2018). Meta-reinforcement learning of structured exploration strategies. In *Advances in Neural Information Processing Systems 31 (NeurIPS-18)*, pages 5302–5311.
- [16] Henderson, P., Chang, W.-D., Shkurti, F., Hansen, J., Meger, D., and Dudek, G. (2017). Benchmark environments for multitask learning in continuous domains. *ICML Lifelong Learning: A Reinforcement Learning Approach Workshop*.
- [17] Huszár, F. (2018). Note on the quadratic penalties in elastic weight consolidation. *Proceedings of the National Academy of Sciences (PNAS)*, pages E2496–E2497.
- [18] Isele, D. and Cosgun, A. (2018). Selective experience replay for lifelong learning. In *Proceedings of the Thirty-Second AAAI Conference on Artificial Intelligence (AAAI-18)*, pages 3302–3309.
- [19] Isele, D., Rostami, M., and Eaton, E. (2016). Using task features for zero-shot knowledge transfer in lifelong learning. In *Proceedings of the Twenty-Fifth International Joint Conference on Artificial Intelligence (IJCAI-16)*, pages 1620–1626.
- [20] Kakade, S. M. (2002). A natural policy gradient. In *Advances in Neural Information Processing Systems 15 (NeurIPS-02)*, pages 1531–1538.
- [21] Kirkpatrick, J., Pascanu, R., Rabinowitz, N., Veness, J., Desjardins, G., Rusu, A. A., Milan, K., Quan, J., Ramalho, T., Grabska-Barwinska, A., et al. (2017). Overcoming catastrophic forgetting in neural networks. *Proceedings of the National Academy of Sciences (PNAS)*, 114(13):3521–3526.
- [22] Li, Z. and Hoiem, D. (2017). Learning without forgetting. *IEEE Transactions on Pattern Analysis and Machine Intelligence (TPAMI)*, 40(12):2935–2947.
- [23] Lillicrap, T. P., Hunt, J. J., Pritzel, A., Heess, N., Erez, T., Tassa, Y., Silver, D., and Wierstra, D. (2016). Continuous control with deep reinforcement learning. In *4th International Conference on Learning Representations (ICLR-16)*.
- [24] McCloskey, M. and Cohen, N. J. (1989). Catastrophic interference in connectionist networks: The sequential learning problem. In *Psychology of Learning and Motivation*, volume 24, pages 109–165. Elsevier.
- [25] Nagabandi, A., Finn, C., and Levine, S. (2019). Deep online learning via meta-learning: Continual adaptation for model-based RL. In *7th International Conference on Learning Representations (ICLR-19)*.
- [26] Nguyen, C. V., Li, Y., Bui, T. D., and Turner, R. E. (2018). Variational continual learning. In *6th International Conference on Learning Representations (ICLR-18)*.
- [27] Parisotto, E., Ba, J. L., and Salakhutdinov, R. (2016). Actor-mimic: Deep multitask and transfer reinforcement learning. In *4th International Conference on Learning Representations (ICLR-16)*.
- [28] Rajeswaran, A., Lowrey, K., Todorov, E. V., and Kakade, S. M. (2017). Towards generalization and simplicity in continuous control. In *Advances in Neural Information Processing Systems 30 (NeurIPS-17)*, pages 6550–6561.
- [29] Ritter, H., Botev, A., and Barber, D. (2018). Online structured Laplace approximations for overcoming catastrophic forgetting. In *Advances in Neural Information Processing Systems 31 (NeurIPS-18)*, pages 3738–3748.
- [30] Rolnick, D., Ahuja, A., Schwarz, J., Lillicrap, T., and Wayne, G. (2019). Experience replay for continual learning. In *Advances in Neural Information Processing Systems 32 (NeurIPS-19)*, pages 348–358.
- [31] Rusu, A. A., Rabinowitz, N. C., Desjardins, G., Soyer, H., Kirkpatrick, J., Kavukcuoglu, K., Pascanu, R., and Hadsell, R. (2016). Progressive neural networks. *arXiv preprint arXiv:1606.04671*.
- [32] Ruvolo, P. and Eaton, E. (2013). ELLA: An efficient lifelong learning algorithm. In *Proceedings of the 30th International Conference on Machine Learning (ICML-13)*, pages 507–515.

- [33] Schulman, J., Levine, S., Abbeel, P., Jordan, M., and Moritz, P. (2015). Trust region policy optimization. In *Proceedings of the 32nd International Conference on Machine Learning (ICML-15)*, pages 1889–1897.
- [34] Schulman, J., Wolski, F., Dhariwal, P., Radford, A., and Klimov, O. (2017). Proximal policy optimization algorithms. *arXiv preprint arXiv:1707.06347*.
- [35] Teh, Y., Bapst, V., Czarnecki, W. M., Quan, J., Kirkpatrick, J., Hadsell, R., Heess, N., and Pascanu, R. (2017). Distal: Robust multitask reinforcement learning. In *Advances in Neural Information Processing Systems 30 (NeurIPS-17)*, pages 4496–4506.
- [36] Titsias, M. K., Schwarz, J., de G. Matthews, A. G., Pascanu, R., and Teh, Y. W. (2020). Functional regularisation for continual learning with Gaussian processes. In *8th International Conference on Learning Representations (ICLR-20)*.
- [37] Van der Vaart, A. (2000). *Asymptotic statistics*, volume 3. Cambridge University Press.
- [38] Yang, Z., Merrick, K. E., Abbass, H. A., and Jin, L. (2017). Multi-task deep reinforcement learning for continuous action control. In *Proceedings of the Twenty-Sixth International Joint Conference on Artificial Intelligence (IJCAI-17)*, pages 3301–3307.
- [39] Yu, T., Quillen, D., He, Z., Julian, R., Hausman, K., Finn, C., and Levine, S. (2019). Meta-World: A benchmark and evaluation for multi-task and meta reinforcement learning. In *Proceedings of the 3rd Conference on Robot Learning (CoRL-19)*.
- [40] Zenke, F., Poole, B., and Ganguli, S. (2017). Continual learning through synaptic intelligence. In *Proceedings of the 34th International Conference on Machine Learning (ICML-17)*, pages 3987–3995.
- [41] Zhao, C., Hospedales, T. M., Stulp, F., and Sigaud, O. (2017). Tensor based knowledge transfer across skill categories for robot control. In *Proceedings of the Twenty-Sixth International Joint Conference on Artificial Intelligence (IJCAI-17)*, pages 3462–3468.

Appendices to “Lifelong Policy Gradient Learning of Factored Policies for Faster Training Without Forgetting”

by Jorge A. Mendez, Boyu Wang, and Eric Eaton

A Proofs of theoretical guarantees

Here, we present complete proofs for the three results on the convergence of LPG-FTW described in Section 5.3 of the main paper. First, recall the definitions of the actual objective we want to maximize:

$$g_t(\mathbf{L}) = \frac{1}{t} \sum_{i=1}^t \max_{\mathbf{s}^{(i)}} \left\{ \|\boldsymbol{\alpha}^{(i)} - \mathbf{L}\mathbf{s}^{(i)}\|_{\mathbf{H}^{(i)}}^2 + \mathbf{g}^{(i)\top} (\mathbf{L}\mathbf{s}^{(i)} - \boldsymbol{\alpha}^{(i)}) - \mu \|\mathbf{s}^{(i)}\|_1 \right\} - \lambda \|\mathbf{L}\|_F^2 ,$$

the surrogate objective we use for optimizing \mathbf{L} :

$$\hat{g}_t(\mathbf{L}) = -\lambda \|\mathbf{L}\|_F^2 + \frac{1}{t} \sum_{i=1}^t \hat{\ell}(\mathbf{L}, \mathbf{s}^{(i)}, \boldsymbol{\alpha}^{(i)}, \mathbf{H}^{(i)}, \mathbf{g}^{(i)}) ,$$

and the expected objective:

$$g(\mathbf{L}) = \mathbb{E}_{\mathbf{H}^{(t)}, \mathbf{g}^{(t)}, \boldsymbol{\alpha}^{(t)}} \left[\max_{\mathbf{s}} \hat{\ell}(\mathbf{L}, \mathbf{s}, \boldsymbol{\alpha}^{(t)}, \mathbf{H}^{(t)}, \mathbf{g}^{(t)}) \right] ,$$

with $\hat{\ell}(\mathbf{L}, \mathbf{s}, \boldsymbol{\alpha}, \mathbf{H}, \mathbf{g}) = -\mu \|\mathbf{s}\|_1 + \|\boldsymbol{\alpha} - \mathbf{L}\mathbf{s}\|_{\mathbf{H}}^2 + \mathbf{g}^\top (\mathbf{L}\mathbf{s} - \boldsymbol{\alpha})$. The convergence results of LPG-FTW are summarized as: 1) the knowledge base \mathbf{L}_t becomes increasingly stable, 2) \hat{g}_t , g_t , and g converge to the same value, and \mathbf{L}_t converges to a stationary point of g . These results, given below as Propositions 1, 2, and 3, are based on the following assumptions:

- A. The tuples $(\mathbf{H}^{(t)}, \mathbf{g}^{(t)})$ are drawn *i.i.d.* from a distribution with compact support.
- B. The sequence $\{\boldsymbol{\alpha}^{(t)}\}_{t=1}^\infty$ is stationary and ϕ -mixing.
- C. The magnitude of $\mathcal{J}^{(t)}(\mathbf{0})$ is bounded by B .
- D. For all \mathbf{L} , $\mathbf{H}^{(t)}$, $\mathbf{g}^{(t)}$, and $\boldsymbol{\alpha}^{(t)}$, the largest eigenvalue (smallest in magnitude) of $\mathbf{L}_\gamma^\top \mathbf{H}^{(t)} \mathbf{L}_\gamma$ is at most -2κ , with $\kappa > 0$, where γ is the set of non-zero indices of $\mathbf{s}^{(t)} = \arg \max_{\mathbf{s}} \hat{\ell}(\mathbf{L}, \mathbf{s}, \mathbf{H}^{(t)}, \mathbf{g}^{(t)}, \boldsymbol{\alpha}^{(t)})$. The non-zero elements of the unique maximizing $\mathbf{s}^{(t)}$ are given by: $\mathbf{s}_\gamma^{(t)} = (\mathbf{L}_\gamma^\top \mathbf{H}^{(t)} \mathbf{L}_\gamma)^{-1} \left(\mathbf{L}^\top (\mathbf{H}^{(t)} \boldsymbol{\alpha}^{(t)} - \mathbf{g}^{(t)}) - \mu \text{sign}(\mathbf{s}_\gamma^{(t)}) \right)$.

Note that the $\boldsymbol{\alpha}^{(t)}$'s are not independently obtained, so we cannot assume they are *i.i.d.* like Ruvolo and Eaton [32]. Therefore, we use a weaker assumption on the sequence of $\boldsymbol{\alpha}^{(t)}$'s found by our algorithm, which enables us to use the Donsker theorem [3] and the Glivenko-Cantelli theorem [2].

Claim 1. $\exists c_1, c_2, c_3 \in \mathbb{R}$ such that no element of \mathbf{L}_t , $\mathbf{s}^{(t)}$, and $\boldsymbol{\alpha}^{(t)}$ has magnitude greater than c_1 , c_2 , and c_3 , respectively, $\forall t \in \{1, \dots, \infty\}$.

Proof. We complete this proof by strong induction. In the base case, \mathbf{L}_1 is given by $\arg \max_{\boldsymbol{\epsilon}} \mathcal{J}^{(1)}(\boldsymbol{\epsilon}) - \lambda \|\boldsymbol{\epsilon}\|_2^2$. If $\boldsymbol{\epsilon} = \mathbf{0}$, the objective becomes $\mathcal{J}^{(1)}(\mathbf{0})$, which is bounded by Assumption C. This implies that if $\boldsymbol{\epsilon}$ grows too large, $-\lambda \|\boldsymbol{\epsilon}\|_2^2$ would be too negative, and then it would not be a maximizer. $\mathbf{s}^{(1)} = \mathbf{1}$ per Algorithm 2, and so $\boldsymbol{\alpha}^{(1)} = \mathbf{L}_1$, which we just showed is bounded.

Then, for $t \leq k$, we have that $\mathbf{s}^{(t)}$ and $\boldsymbol{\epsilon}^{(t)}$ are given by $\arg \max_{\mathbf{s}, \boldsymbol{\epsilon}} \mathcal{J}^{(t)}(\mathbf{L}_{t-1}\mathbf{s} + \boldsymbol{\epsilon}) - \mu \|\mathbf{s}\|_1 - \lambda \|\boldsymbol{\epsilon}\|_2^2$. If $\mathbf{s} = \mathbf{0}$ and $\boldsymbol{\epsilon} = \mathbf{0}$, this becomes $\mathcal{J}^{(t)}(\mathbf{0})$, which is again bounded, and therefore neither $\boldsymbol{\epsilon}$ nor \mathbf{s} may grow too large. The bound on $\boldsymbol{\alpha}^{(t)}$ follows by induction, since $\boldsymbol{\alpha}^{(t)} = \mathbf{L}_{t-1}\mathbf{s}^{(t)}$. Moreover, since only the t -th column of \mathbf{L} is modified by setting it to $\boldsymbol{\epsilon}$, \mathbf{L}_t is also bounded. For $t > k$, the same argument applies to $\mathbf{s}^{(t)}$ and therefore to $\boldsymbol{\alpha}^{(t)}$. \mathbf{L}_t is then given by $\arg \max_{\mathbf{L}} -\lambda \|\mathbf{L}\|_F^2 +$

$\frac{1}{t} \sum_{\hat{t}}^t \|Ls^{(\hat{t})} - \alpha^{(\hat{t})}\|_{H^{(\hat{t})}}^2 + g^{(\hat{t})\top} (Ls^{(\hat{t})} - \alpha^{(\hat{t})})$. If $L_t = \mathbf{0}$, the objective for task \hat{t} becomes $\alpha^{(\hat{t})\top} H^{(\hat{t})} \alpha^{(\hat{t})} + g^{(\hat{t})\top} \alpha^{(\hat{t})}$. By Assumption A and strong induction, this is bounded for all $\hat{t} \leq t$, so if any element of L is too large, L would not be a maximizer because of the regularization term. ■

Proposition 1. $L_t - L_{t-1} = O(\frac{1}{t})$.

Proof. First, we show that $\hat{g}_t - \hat{g}_{t-1}$ is Lipschitz with constant $O(\frac{1}{t})$. To show this, we note that $\hat{\ell}$ is Lipschitz in L with a constant independent of t , since it is a quadratic function over a compact region with bounded coefficients. Next, we have:

$$\begin{aligned} \hat{g}_t(L) - \hat{g}_{t-1}(L) &= \frac{1}{t} \hat{\ell}(L, s^{(t)}, \alpha^{(t)}, H^{(t)}, g^{(t)}) + \frac{1}{t} \sum_{\hat{t}=1}^{t-1} \hat{\ell}(L, s^{(\hat{t})}, \alpha^{(\hat{t})}, H^{(\hat{t})}, g^{(\hat{t})}) \\ &\quad - \frac{1}{t-1} \sum_{\hat{t}=1}^{t-1} \hat{\ell}(L, s^{(\hat{t})}, \alpha^{(\hat{t})}, H^{(\hat{t})}, g^{(\hat{t})}) \\ &= \frac{1}{t} \hat{\ell}(L, s^{(t)}, \alpha^{(t)}, H^{(t)}, g^{(t)}) + \frac{1}{t(t-1)} \sum_{\hat{t}=1}^{t-1} \hat{\ell}(L, s^{(\hat{t})}, \alpha^{(\hat{t})}, H^{(\hat{t})}, g^{(\hat{t})}) . \end{aligned}$$

Therefore, $\hat{g}_t - \hat{g}_{t-1}$ has a Lipschitz constant $O(\frac{1}{t})$, since it is the difference of two terms divided by t : $\hat{\ell}$ and an average over $t-1$ terms, whose Lipschitz constant is bounded by the largest Lipschitz constant of the terms.

Let ξ_t be the Lipschitz constant of $\hat{g}_t - \hat{g}_{t-1}$. We have:

$$\begin{aligned} \hat{g}_{t-1}(L_{t-1}) - \hat{g}_{t-1}(L_t) &= \hat{g}_{t-1}(L_{t-1}) - \hat{g}_t(L_{t-1}) + \hat{g}_t(L_{t-1}) - \hat{g}_t(L_t) + \hat{g}_t(L_t) - \hat{g}_{t-1}(L_t) \\ &\leq \hat{g}_{t-1}(L_{t-1}) - \hat{g}_t(L_{t-1}) + \hat{g}_t(L_t) - \hat{g}_{t-1}(L_t) \\ &= -(\hat{g}_t - \hat{g}_{t-1})(L_{t-1}) + (\hat{g}_t - \hat{g}_{t-1})(L_t) \leq \xi_t \|L_t - L_{t-1}\|_F . \end{aligned}$$

Moreover, since L_{t-1} maximizes \hat{g}_{t-1} and the ℓ_2 regularization term ensures that the maximum eigenvalue of the Hessian of \hat{g}_{t-1} is upper-bounded by -2λ , we have that $\hat{g}_{t-1}(L_{t-1}) - \hat{g}_{t-1}(L_t) \geq \lambda \|L_t - L_{t-1}\|_F^2$. Combining these two inequalities, we have: $\|L_t - L_{t-1}\|_F \leq \frac{\xi_t}{\lambda} = O(\frac{1}{t})$. ■

The critical step for adapting the proof from Ruvolo and Eaton [32] to LPG-FTW is to introduce the following lemma, which shows the equality of the maximizers of ℓ and $\hat{\ell}$.

Lemma 1. $\hat{\ell}(L_t, s^{(t+1)}, \alpha^{(t+1)}, H^{(t+1)}, g^{(t+1)}) = \max_s \hat{\ell}(L_t, s, \alpha^{(t+1)}, H^{(t+1)}, g^{(t+1)})$.

Proof. To show this, we need the following to hold:

$$s^{(t+1)} = \arg \max_s \ell(L_t, s) = \arg \max_s \hat{\ell}(L_t, s, \alpha^{(t+1)}, H^{(t+1)}, g^{(t+1)}) .$$

We first compute the gradient of ℓ , given by:

$$\nabla_s \ell(L_t, s) = -\mu \text{sign}(s) + L_t^\top \nabla_{\theta} \mathcal{J}^{(t+1)}(\theta) \Big|_{\theta=L_t s} .$$

Since $s^{(t+1)}$ is the maximizer of ℓ , we have:

$$\nabla_s \ell(L_t, s) \Big|_{s=s^{(t+1)}} = -\mu \text{sign}(s^{(t+1)}) + L_t^\top g^{(t+1)} = \mathbf{0} . \quad (\text{A.1})$$

We now compute the gradient of $\hat{\ell}$ and evaluate it at $s^{(t+1)}$:

$$\begin{aligned} \nabla_s \hat{\ell}(L_t, s, \alpha^{(t+1)}, H^{(t+1)}, g^{(t+1)}) &= -\mu \text{sign}(s^{(t+1)}) + L_t g^{(t+1)} - 2L_t^\top H^{(t+1)} (\alpha^{(t+1)} - L_t s) \\ \nabla_s \hat{\ell}(L_t, s, \alpha^{(t+1)}, H^{(t+1)}, g^{(t+1)}) \Big|_{s=s^{(t+1)}} &= -\mu \text{sign}(s^{(t+1)}) + L_t^\top g^{(t+1)} = \mathbf{0} , \end{aligned}$$

since it matches Equation A.1. By Assumption D, $\hat{\ell}$ has a unique maximizer $s^{(t+1)}$. ■

Before stating our next lemma, we define:

$$\mathbf{s}^* = \beta(\mathbf{L}, \boldsymbol{\alpha}^{(t)}, \mathbf{H}^{(t)}, \mathbf{g}^{(t)}) = \arg \max_{\mathbf{s}} \hat{\ell}(\mathbf{L}, \mathbf{s}, \boldsymbol{\alpha}^{(t)}, \mathbf{H}^{(t)}, \mathbf{g}^{(t)}) .$$

Lemma 2.

- A. $\max_{\mathbf{s}} \hat{\ell}(\mathbf{L}, \mathbf{s}, \boldsymbol{\alpha}^{(t)}, \mathbf{H}^{(t)}, \mathbf{g}^{(t)})$ is continuously differentiable in \mathbf{L} with $\nabla_{\mathbf{L}} \max_{\mathbf{s}} \hat{\ell}(\mathbf{L}, \mathbf{s}, \boldsymbol{\alpha}^{(t)}, \mathbf{H}^{(t)}, \mathbf{g}^{(t)}) = \left[-2\mathbf{H}^{(t)}\mathbf{s}^* + \mathbf{g}^{(t)} \right] \mathbf{s}^{*\top}$.
- B. g is continuously differentiable and $\nabla_{\mathbf{L}} g(\mathbf{L}) = -2\lambda \mathbf{I} + \mathbb{E} \left[\nabla_{\mathbf{L}} \max_{\mathbf{s}} \hat{\ell}(\mathbf{L}, \mathbf{s}, \boldsymbol{\alpha}^{(t)}, \mathbf{H}^{(t)}, \mathbf{g}^{(t)}) \right]$.
- C. $\nabla_{\mathbf{L}} g(\mathbf{L})$ is Lipschitz in the space of latent components \mathbf{L} that obey Claim 1.

Proof. To prove Part A, we apply a corollary to Theorem 4.1 in [4]. This corollary states that if $\hat{\ell}$ is continuously differentiable in \mathbf{L} (which it clearly is) and has a unique maximizer $\mathbf{s}^{(t)}$ (which is guaranteed by Assumption D), then $\nabla_{\mathbf{L}} \max_{\mathbf{s}} \hat{\ell}(\mathbf{L}, \mathbf{s}, \boldsymbol{\alpha}^{(t)}, \mathbf{H}^{(t)}, \mathbf{g}^{(t)})$ exists and is equal to $\nabla_{\mathbf{L}} \hat{\ell}(\mathbf{L}, \mathbf{s}^*, \boldsymbol{\alpha}^{(t)}, \mathbf{H}^{(t)}, \mathbf{g}^{(t)})$, given by $\left[-2\mathbf{H}^{(t)}\mathbf{s}^* + \mathbf{g}^{(t)} \right] \mathbf{s}^{*\top}$. Part B follows since by Assumption A and Claim 1 the tuple $(\mathbf{H}^{(t)}, \mathbf{g}^{(t)}, \boldsymbol{\alpha}^{(t)})$ is drawn from a distribution with compact support.

To prove Part C, we first show that β is Lipschitz in \mathbf{L} with constant independent of $\boldsymbol{\alpha}^{(t)}$, $\mathbf{H}^{(t)}$, and $\mathbf{g}^{(t)}$. Part C will follow due to the form of the gradient of g with respect to \mathbf{L} . The function β is continuous in its arguments since $\hat{\ell}$ is continuous in its arguments and by Assumption D has a unique maximizer. Next, we define $\rho(\mathbf{L}, \mathbf{H}^{(t)}, \mathbf{g}^{(t)}, \boldsymbol{\alpha}^{(t)}, j) = \mathbf{l}_j^\top \left[2\mathbf{H}^{(t)}(\mathbf{L}\mathbf{s}^* - \boldsymbol{\alpha}^{(t)}) + \mathbf{g}^{(t)} \right]$, where \mathbf{l}_j is the j -th column of \mathbf{L} . Following the argument of Fuchs [13], we reach the following conditions:

$$\begin{aligned} \left| \rho(\mathbf{L}, \mathbf{H}^{(t)}, \mathbf{g}^{(t)}, \boldsymbol{\alpha}^{(t)}, j) \right| = \mu &\iff \mathbf{s}_j^* \neq 0 \\ \left| \rho(\mathbf{L}, \mathbf{H}^{(t)}, \mathbf{g}^{(t)}, \boldsymbol{\alpha}^{(t)}, j) \right| < \mu &\iff \mathbf{s}_j^* = 0 . \end{aligned} \quad (\text{A.2})$$

Let γ be the set of indices j such that $\left| \rho(\mathbf{L}, \mathbf{H}^{(t)}, \mathbf{g}^{(t)}, \boldsymbol{\alpha}^{(t)}, j) \right| = \mu$. Since ρ is continuous in \mathbf{L} , $\mathbf{H}^{(t)}$, $\mathbf{g}^{(t)}$, and $\boldsymbol{\alpha}^{(t)}$, there must exist an open neighborhood V around $(\mathbf{L}, \mathbf{H}^{(t)}, \mathbf{g}^{(t)}, \boldsymbol{\alpha}^{(t)})$ such that for all $(\mathbf{L}', \mathbf{H}^{(t)'}, \mathbf{g}^{(t)'}, \boldsymbol{\alpha}^{(t)'}) \in V$ and $j \notin \gamma$, $\left| \rho(\mathbf{L}', \mathbf{H}^{(t)'}, \mathbf{g}^{(t)'}, \boldsymbol{\alpha}^{(t)'}, j) \right| < \mu$. By Equation A.2, we conclude that $\beta(\mathbf{L}', \mathbf{H}^{(t)'}, \mathbf{g}^{(t)'}, \boldsymbol{\alpha}^{(t)'})_j = 0, \forall j \notin \gamma$.

Next, we define a new objective:

$$\bar{\ell}(\mathbf{L}_\gamma, \mathbf{s}_\gamma, \boldsymbol{\alpha}, \mathbf{H}, \mathbf{g}) = \|\boldsymbol{\alpha} - \mathbf{L}_\gamma \mathbf{s}_\gamma\|_{\mathbf{H}}^2 + \mathbf{g}^\top (\mathbf{L}_\gamma \mathbf{s}_\gamma - \boldsymbol{\alpha}) - \mu \|\mathbf{s}_\gamma\|_1 .$$

By Assumption D, $\bar{\ell}$ is strictly concave with a Hessian upper-bounded by -2κ . We can conclude that:

$$\begin{aligned} \bar{\ell}(\mathbf{L}_\gamma, \beta(\mathbf{L}, \boldsymbol{\alpha}^{(t)}, \mathbf{H}^{(t)}, \mathbf{g}^{(t)})_\gamma, \boldsymbol{\alpha}^{(t)}, \mathbf{H}^{(t)}, \mathbf{g}^{(t)}) - \bar{\ell}(\mathbf{L}_\gamma, \beta(\mathbf{L}', \boldsymbol{\alpha}^{(t)'}, \mathbf{H}^{(t)'}, \mathbf{g}^{(t)'})_\gamma, \boldsymbol{\alpha}^{(t)}, \mathbf{H}^{(t)}, \mathbf{g}^{(t)}) \\ \geq \kappa \left\| \beta(\mathbf{L}', \boldsymbol{\alpha}^{(t)'}, \mathbf{H}^{(t)'}, \mathbf{g}^{(t)'})_\gamma - \beta(\mathbf{L}, \boldsymbol{\alpha}^{(t)}, \mathbf{H}^{(t)}, \mathbf{g}^{(t)})_\gamma \right\|_2^2 . \end{aligned} \quad (\text{A.3})$$

On the other hand, by Assumption A and Claim 1, $\bar{\ell}$ is Lipschitz in its second argument with constant $e_1 \|\mathbf{L}_\gamma - \mathbf{L}'_\gamma\|_{\mathbf{F}} + e_2 \|\boldsymbol{\alpha} - \boldsymbol{\alpha}'\|_2 + e_3 \|\mathbf{H} - \mathbf{H}'\|_{\mathbf{F}} + e_4 \|\mathbf{g} - \mathbf{g}'\|_2$, where e_{1-4} are all constants independent of any of the arguments. Combining this with Equation A.3, we obtain:

$$\begin{aligned} \left\| \beta(\mathbf{L}', \boldsymbol{\alpha}^{(t)'}, \mathbf{H}^{(t)'}, \mathbf{g}^{(t)'}) - \beta(\mathbf{L}, \boldsymbol{\alpha}^{(t)}, \mathbf{H}^{(t)}, \mathbf{g}^{(t)}) \right\| &= \\ \left\| \beta(\mathbf{L}', \boldsymbol{\alpha}^{(t)'}, \mathbf{H}^{(t)'}, \mathbf{g}^{(t)'})_\gamma - \beta(\mathbf{L}, \boldsymbol{\alpha}^{(t)}, \mathbf{H}^{(t)}, \mathbf{g}^{(t)})_\gamma \right\| & \\ \leq \frac{e_1 \|\mathbf{L}_\gamma - \mathbf{L}'_\gamma\|_{\mathbf{F}} + e_2 \|\boldsymbol{\alpha}^{(t)} - \boldsymbol{\alpha}^{(t)'}\|_2}{\kappa} + \frac{e_3 \|\mathbf{H}^{(t)} - \mathbf{H}^{(t)'}\|_{\mathbf{F}} + e_4 \|\mathbf{g}^{(t)} - \mathbf{g}^{(t)'}\|_2}{\kappa} . \end{aligned}$$

Therefore, β is locally Lipschitz. Since the domain of β is compact by Assumption A and Claim 1, this implies that β is uniformly Lipschitz, and we can conclude that ∇g is Lipschitz as well. \blacksquare

Proposition 2.

1. $\hat{g}_t(\mathbf{L}_t)$ converges a.s.
2. $g_t(\mathbf{L}_t) - \hat{g}_t(\mathbf{L}_t)$ converges a.s. to 0
3. $g_t(\mathbf{L}_t) - \hat{g}_t(\mathbf{L}_t)$ converges a.s. to 0
4. $g(\mathbf{L}_t)$ converges a.s.

Proof. We begin by defining the stochastic process $u_t = \hat{g}_t(\mathbf{L})$. The outline of the proof is to show that this process is a quasi-martingale and by a theorem by Fisk [12], it converges almost surely.

$$\begin{aligned}
u_{t+1} - u_t &= \hat{g}_{t+1}(\mathbf{L}_{t+1}) - \hat{g}_t(\mathbf{L}_t) = \hat{g}_{t+1}(\mathbf{L}_{t+1}) - \hat{g}_{t+1}(\mathbf{L}_t) + \hat{g}_{t+1}(\mathbf{L}_t) - \hat{g}_t(\mathbf{L}_t) \\
&= (\hat{g}_{t+1}(\mathbf{L}_{t+1}) - \hat{g}_{t+1}(\mathbf{L}_t)) + \frac{g_t(\mathbf{L}_t) - \hat{g}_t(\mathbf{L}_t)}{t+1} \\
&\quad + \frac{\max_{\mathbf{s}} \hat{\ell}(\mathbf{L}_t, \mathbf{s}, \boldsymbol{\alpha}^{(t+1)}, \mathbf{H}^{(t+1)}, \mathbf{g}^{(t+1)})}{t+1} - \frac{g_t(\mathbf{L}_t)}{t+1} ,
\end{aligned} \tag{A.4}$$

where we made use of the fact that:

$$\begin{aligned}
\hat{g}_{t+1}(\mathbf{L}_t) &= \frac{\hat{\ell}(\mathbf{L}_t, \mathbf{s}^{(t+1)}, \boldsymbol{\alpha}^{(t+1)}, \mathbf{H}^{(t+1)}, \mathbf{g}^{(t+1)})}{t+1} + \frac{t}{t+1} \hat{g}_t(\mathbf{L}_t) \\
&= \frac{\max_{\mathbf{s}} \hat{\ell}(\mathbf{L}_t, \mathbf{s}, \boldsymbol{\alpha}^{(t+1)}, \mathbf{H}^{(t+1)}, \mathbf{g}^{(t+1)})}{t+1} + \frac{t}{t+1} \hat{g}_t(\mathbf{L}_t) ,
\end{aligned}$$

where the second equality holds by Lemma 1.

We now need to show that the sum of positive and negative variations in Equation A.4 are bounded. By an argument similar to a lemma by Bottou [5], the sum of positive variations of u_t is bounded, since \hat{g} is upper-bounded by Assumption C. Therefore, it suffices to show that the sum of negative variations is bounded. The first term on the first line of Equation A.4 is guaranteed to be positive since \mathbf{L}_{t+1} maximizes \hat{g}_{t+1} . Additionally, since g_t is always at least as large as \hat{g}_t , the second term on the first line is also guaranteed to be positive. Therefore, we focus on the second line.

$$\begin{aligned}
\mathbb{E}[u_{t+1} - u_t \mid \mathcal{I}_t] &\geq \frac{\mathbb{E}[\max_{\mathbf{s}} \hat{\ell}(\mathbf{L}_t, \mathbf{s}, \boldsymbol{\alpha}^{(t+1)}, \mathbf{H}^{(t+1)}, \mathbf{g}^{(t+1)}) \mid \mathcal{I}_t]}{t+1} - \frac{g_t(\mathbf{L}_t)}{t+1} \\
&= \frac{g(\mathbf{L}_t) - g_t(\mathbf{L}_t)}{t+1} \geq -\frac{\|g - g_t\|_{\infty}}{t+1} ,
\end{aligned}$$

where \mathcal{I}_t represents all the $\boldsymbol{\alpha}^{(i)}$'s, $\mathbf{H}^{(i)}$'s, and $\mathbf{g}^{(i)}$'s up to time t . Hence, showing that $\sum_{t=1}^{\infty} \frac{\|g - g_t\|_{\infty}}{t+1} < \infty$ will prove that u_t is a quasi-martingale that converges almost surely.

In order to prove this, we apply the following corollary of the Donsker theorem [37]:

Let $\mathcal{F} = \{f_{\boldsymbol{\theta}} : \mathcal{X} \mapsto \mathbb{R}, \boldsymbol{\theta} \in \Theta\}$ be a set of measurable functions indexed by a bounded subset Θ of \mathbb{R}^d . Suppose that there exists a constant K such that:

$$|f_{\boldsymbol{\theta}_1}(x) - f_{\boldsymbol{\theta}_2}(x)| \leq K \|\boldsymbol{\theta}_1 - \boldsymbol{\theta}_2\|_2$$

for every $\boldsymbol{\theta}_1, \boldsymbol{\theta}_2 \in \Theta$ and $x \in \mathcal{X}$. Then, \mathcal{F} is P-Donsker and for any $f \in \mathcal{F}$, we define:

$$\begin{aligned}
\mathbb{P}_n f &= \frac{1}{n} \sum_{i=1}^n f(X_i) \\
\mathbb{P} f &= \mathbb{E}_X[f(X)] \\
\mathbb{G}_n f &= \sqrt{n}(\mathbb{P}_n f - \mathbb{P} f) .
\end{aligned}$$

If $\mathbb{P} f^2 \leq \delta^2$ and $\|f\|_{\infty} < B$ and the random elements are Borel measurable, then:

$$\mathbb{E}[\sup_{f \in \mathcal{F}} |\mathbb{G}_n f|] = O(1) .$$

In order to apply this corollary to our analysis, consider a set of functions \mathcal{F} indexed by \mathbf{L} , given by $f_{\mathbf{L}}(\mathbf{H}^{(t)}, \mathbf{g}^{(t)}, \boldsymbol{\alpha}^{(t)}) = \max_{\mathbf{s}} \hat{\ell}(\mathbf{L}, \mathbf{s}, \boldsymbol{\alpha}^{(t)}, \mathbf{H}^{(t)}, \mathbf{g}^{(t)})$, whose domain is all possible tuples $(\mathbf{H}^{(t)}, \mathbf{g}^{(t)}, \boldsymbol{\alpha}^{(t)})$. The expected value of f^2 is bounded for all $f \in \mathcal{F}$ since $\hat{\ell}$ is bounded by

Claim 1. Second, $\|f\|_\infty$ is bounded given Claim 1 and Assumption A. Finally, by Assumptions A and B, the corollary applies to the tuples $(\mathbf{H}^{(t)}, \mathbf{g}^{(t)}, \boldsymbol{\alpha}^{(t)})$ [3]. Therefore, we can state that:

$$\mathbb{E} \left[\sqrt{t} \left\| \left(\frac{1}{t} \sum_{\hat{t}=1}^t \max_{\mathbf{s}} \hat{\ell}(\mathbf{L}, \mathbf{s}, \boldsymbol{\alpha}^{(\hat{t})}, \mathbf{H}^{(\hat{t})}, \mathbf{g}^{(\hat{t})}) \right) - \mathbb{E} \left[\max_{\mathbf{s}} \hat{\ell}(\mathbf{L}, \mathbf{s}, \boldsymbol{\alpha}^{(t)}, \mathbf{H}^{(t)}, \mathbf{g}^{(t)}) \right] \right\|_\infty \right] = O(1)$$

$$\implies \mathbb{E}[\|\mathbf{g}_t(\mathbf{L}) - \mathbf{g}(\mathbf{L})\|_\infty] = O\left(\frac{1}{\sqrt{t}}\right).$$

Therefore, $\exists c_3 \in \mathbb{R}$ such that $\mathbb{E}[\|\mathbf{g}_t - \mathbf{g}\|_\infty] < \frac{c_3}{\sqrt{t}}$:

$$\sum_{t=1}^{\infty} \mathbb{E}[\mathbb{E}[u_{t+1} - u_t \mid \mathcal{I}_t]^-] \geq \sum_{t=1}^{\infty} -\frac{\mathbb{E}[\|\mathbf{g}_t - \mathbf{g}\|_\infty]}{t+1} > \sum_{t=1}^{\infty} -\frac{c_3}{t^{\frac{3}{2}}} = -O(1),$$

where $i^- = \min(i, 0)$. This shows that the sum of negative variations of u_t is bounded, so u_t is a quasi-martingale and thus converges almost surely [12]. This proves Part 1 of Proposition 2.

Next, we show that u_t being a quasi-martingale implies the almost sure convergence of the fourth line of Equation A.4. To see this, we note that since u_t is a quasi-martingale and the sum of its positive variations is bounded, and since the term on the fourth line of Equation A.4, $\frac{g_t(\mathbf{L}_t) - \hat{g}_t(\mathbf{L}_t)}{t+1}$, is guaranteed to be positive, the sum of that term from 1 to infinity must be bounded:

$$\sum_{t=1}^{\infty} \frac{g_t(\mathbf{L}_t) - \hat{g}_t(\mathbf{L}_t)}{t+1} < \infty. \quad (\text{A.5})$$

To complete the proof of Part 2 of Proposition 2, consider the following lemma: Let a_n, b_n be two real sequences such that for all n , $a_n \geq 0, b_n \geq 0, \sum_{j=1}^{\infty} a_j = \infty, \sum_{j=1}^{\infty} a_j b_j < \infty, \exists K > 0$ such that $|b_{n+1} - b_n| < K a_n$. Then, $\lim_{n \rightarrow \infty} b_n = 0$. If we define $a_t = \frac{1}{t+1}$ and $b_t = g_t(\mathbf{L}_t) - \hat{g}_t(\mathbf{L}_t)$, then clearly these are both positive sequences and $\sum_{t=1}^{\infty} a_t = \infty$. By Equation A.5, $\sum_{t=1}^{\infty} a_t b_t < \infty$. Finally, since g_t and \hat{g}_t are bounded and Lipschitz with constant independent of t and $\mathbf{L}_{t+1} - \mathbf{L}_t = O(\frac{1}{t})$, we have all of the assumptions verified, which implies that $g_t - \hat{g}_t$ converges a.s. to 0.

By Part 2 and the Glivenko-Cantelli theorem, $\lim_{t \rightarrow \infty} \|\mathbf{g} - \mathbf{g}_t\|_\infty = 0$, which implies that \mathbf{g} must converge almost surely. By transitivity, $\lim_{t \rightarrow \infty} \mathbf{g}(\mathbf{L}_t) - \hat{g}_t(\mathbf{L}_t) = 0$, showing Parts 3 and 4. ■

Proposition 3. *The distance between \mathbf{L}_t and the set of all stationary points of g converges a.s. to 0.*

Proof. First, $\nabla_{\mathbf{L}} \hat{g}_t$ is Lipschitz with a constant independent of t , since the gradient of \hat{g}_t is linear, $\mathbf{s}^{(t)}, \mathbf{H}^{(t)}, \mathbf{g}^{(t)}$, and $\boldsymbol{\alpha}^{(t)}$ are bounded, and the summation in \hat{g}_t is normalized by t . Next, we define an arbitrary non-zero matrix \mathbf{U} of the same dimensionality as \mathbf{L} . Since g_t upper-bounds \hat{g}_t , we have:

$$g_t(\mathbf{L}_t + \mathbf{U}) \geq \hat{g}_t(\mathbf{L}_t + \mathbf{U}) \implies \lim_{t \rightarrow \infty} g(\mathbf{L}_t + \mathbf{U}) \geq \lim_{t \rightarrow \infty} \hat{g}_t(\mathbf{L}_t + \mathbf{U}),$$

where we used the fact that $\lim_{t \rightarrow \infty} g_t = \lim_{t \rightarrow \infty} g$. Let $h_t > 0$ be a sequence of positive real numbers that converges to 0. If we take the first order Taylor expansion on both sides of the inequality and use the fact that ∇g and $\nabla \hat{g}$ are both Lipschitz with constant independent of t , we get:

$$\lim_{t \rightarrow \infty} g_t(\mathbf{L}_t) + \text{Tr}(h_t \mathbf{U}^\top \nabla g_t(\mathbf{L}_t)) + O(h_t \mathbf{U}) \geq \lim_{t \rightarrow \infty} \hat{g}_t(\mathbf{L}_t) + \text{Tr}(h_t \mathbf{U}^\top \nabla \hat{g}_t(\mathbf{L}_t)) + O(h_t \mathbf{U}).$$

Since $\lim_{t \rightarrow \infty} \mathbf{g}(\mathbf{L}_t) - \hat{g}_t(\mathbf{L}_t) = 0$ a.s. and $\lim_{t \rightarrow \infty} h_t = 0$, we have:

$$\lim_{t \rightarrow \infty} \left(\frac{1}{\|\mathbf{U}\|_F} \mathbf{U}^\top \nabla g(\mathbf{L}_t) \right) \geq \lim_{t \rightarrow \infty} \left(\frac{1}{\|\mathbf{U}\|_F} \mathbf{U}^\top \nabla \hat{g}(\mathbf{L}_t) \right).$$

Since this inequality has to hold for every \mathbf{U} , we require that $\lim_{t \rightarrow \infty} \nabla g(\mathbf{L}_t) = \lim_{t \rightarrow \infty} \nabla \hat{g}_t(\mathbf{L}_t)$. Since \mathbf{L}_t minimizes \hat{g}_t , we require that $\nabla \hat{g}_t(\mathbf{L}_t) = \mathbf{0}$. This implies that $\nabla g(\mathbf{L}_t) = \mathbf{0}$, which is a sufficient first-order condition for \mathbf{L}_t to be stationary point of g . ■

B Experimental setting

This section provides additional details of the experimental setting used to arrive at the results presented in Sections 5.1 and 5.2 in the main paper. Table B.1 summarizes the hyper-parameters of all algorithms used for our experiments.

Table B.1: Summary of hyper-parameters. The first digit in EWC versions differentiates variants with shared σ (1) and task-specific σ (2), and the second digit differentiates between Huszár regularization (1), EWC regularization scaled by $\frac{1}{t-1}$ (2), and the original EWC regularization (3). The boldfaced version of EWC was used for our experiments in the paper.

	Hyper-parameter	HC-G	HC-BP	Ho-G	Ho-BP	W-G	W-B	MT10/50
NPG	# iterations	50	50	100	100	200	200	200
	# trajectories	10	10	50	50	50	50	50
	step size	0.5	0.5	0.005	0.005	0.05	0.05	0.005
	λ (GAE)	0.97	0.97	0.97	0.97	0.97	0.97	0.97
	γ (MDP)	0.995	0.995	0.995	0.995	0.995	0.995	0.995
LPG-FTW	λ	$1e-5$	$1e-5$	$1e-5$	$1e-5$	$1e-5$	$1e-5$	$1e-5$
	μ	$1e-5$	$1e-5$	$1e-5$	$1e-5$	$1e-5$	$1e-5$	$1e-5$
	k	5	5	5	5	5	10	3
PG-ELLA	λ	$1e-5$	$1e-5$	$1e-5$	$1e-5$	$1e-5$	$1e-5$	$1e-5$
	μ	$1e-5$	$1e-5$	$1e-5$	$1e-5$	$1e-5$	$1e-5$	$1e-5$
	k	5	5	5	5	5	10	3
EWC 1, 1	λ	$1e-3$	$1e-6$	$1e-7$	$1e-7$	$1e-4$	$1e-5$	—
EWC 1, 2	λ	$1e-3$	$1e-4$	$1e-7$	$1e-3$	$1e-3$	$1e-7$	—
EWC 1, 3	λ	$1e-6$	$1e-6$	$1e-7$	$1e-4$	$1e-7$	$1e-7$	—
EWC 2, 1	λ	$1e-6$	$1e-5$	$1e-6$	$1e-7$	$1e-4$	$1e-4$	—
EWC 2, 2	λ	$1e-4$	$1e-3$	$1e-5$	$1e-7$	$1e-4$	$1e-6$	—
EWC 2, 3	λ	$1e-4$	$1e-4$	$1e-6$	$1e-7$	$1e-4$	$1e-4$	$1e-7$

OpenAI Gym MuJoCo domains The hyper-parameters for NPG were manually selected by running an evaluation on the nominal task for each domain (without gravity or body part modifications). We tried various combinations of the number of iterations, number of trajectories per iteration, and step size, until we reached a learning curve that was fast and reached proficiency. Once these hyper-parameters were found, they were used all lifelong learning algorithms. For LPG-FTW, we chose typical hyper-parameters and held them fixed through all experiments, forgoing potential additional benefits from a hyper-parameter search. The only exception was the number of latent components used for the Walker-2D *body-parts* domain, as we found empirically that $k = 5$ led to saturation of the learning process early on. For PG-ELLA, we kept the same hyper-parameters as used for LPG-FTW, since they are used in exactly the same way for both methods. Finally, for EWC, we ran a grid search over the value of the regularization term, λ , among $\{1e-7, 1e-6, 1e-5, 1e-4, 1e-3\}$. The search was done by running five consecutive tasks for fifty iterations over five trials with different random seeds. We chose λ independently for each domain to maximize the average performance after all tasks had been trained. We also tried various versions of EWC, as described in Appendix D, modifying the regularization term and selecting whether to share the policy’s variance across tasks. The only version that worked in all domains was the original EWC penalty with a shared variance across tasks, so results in the main paper are based on that version. To make comparisons fair, EWC used the full Hessian instead of the diagonal Hessian proposed by the authors.

Meta-World domains In this case, we manually tuned the hyper-parameters for NPG on the *reach* task, which we considered to be the easiest to solve in the benchmark, and again kept those fixed for all lifelong learners. We chose typical values for LPG-FTW for k , λ , and μ , and reused those for PG-ELLA. We used fewer latent components ($k = 3$), since MT10 contains only $T_{\max} = 10$ tasks and we considered that using more than three policy factors would give our algorithm an unfair advantage over single-model methods. For EWC, we ran a grid search for the regularization hyper-parameter in the same way as for the previous experiments. For ER, we used a 50-50 ratio of experience replay as suggested by Rolnick et al. [30], and ensured that each batch sampled from the replay buffer had the same number of trajectories from each previous task. LPG-FTW, PG-ELLA, and EWC all had access to the full Hessian, and we chose for EWC not to share the variance across tasks since the outputs of the policies were task-specific. We ran all Meta-World tasks on version 1.5 of the MuJoCo physics simulator, to match the remainder of our experimental setting. We used the robot hand and the object location (6-D) as the observation space for all tasks. Note that the goal, which was kept fixed for each task, was not given to the agent. For this reason, we removed 2 tasks from MT50 that use at least 9-D observations—*stick pull* and *stick push*—for a total of $T_{\max} = 48$ tasks.

C Diversity of simple domains

One important question in the study of lifelong RL is how diverse the tasks used for evaluation are. To measure this in the OpenAI Gym MuJoCo domains, we evaluated each task’s performance using the final policy trained by LPG-FTW on the correct task and compared it to the average performance using the policies trained on all other tasks. Figure C.1 shows that the policies do not work well across different tasks, demonstrating that the tasks are diverse. Moreover, the most highly-varying domains, Hopper and Walker-2D *body-parts*, are precisely those for which EWC struggled the most, suffering from catastrophic forgetting, as shown in Figure 2 in the paper. This is consistent with the fact that a single policy does not work across various tasks. In those domains, LPG-FTW reached the performance of STL with a high speedup while retaining knowledge from early tasks.

D EWC additional results

During our evaluations on the OpenAI MuJoCo domains, we experimented with six different variants of EWC, by varying two different choices. The first choice was whether to share the variance of the Gaussian policies across the different tasks or not. Sharing the variance enables the algorithm to start from a more deterministic policy, thereby achieving higher initial performance, at the cost of reducing task-specific exploration. The second choice was the exact form of the regularization penalty. In the original EWC formulation, the regularization term applied to the PG objective was $-\lambda \sum_{i=1}^{t-1} \|\theta - \alpha^{(i)}\|_{H^{(i)}}^2$. Huszár [17] noted that this does not correspond to the correct Bayesian formulation, and proposed to instead use $-\lambda \|\theta - \alpha^{(t-1)}\|_{H^{(t-1)}}^2$, where $\alpha^{(t-1)}$ and $H^{(t-1)}$ capture all the information from tasks 1 through $t-1$ in the Bayesian setting. We experimented with these two choices of regularization, plus an additional one where λ is scaled by $\frac{1}{t-1}$ in order for the penalty not to increase linearly with the number of tasks. For all versions, we independently tuned the hyper-parameters as described in Appendix B.

Table D.1 summarizes the results obtained for each variant of EWC. The only version that consistently learned each task’s policy (tune) was the original EWC regularization with the variance shared across tasks. This was also the only variant for which the final performance was never unreasonably low. Therefore, we used this version for all experiments in the main paper.

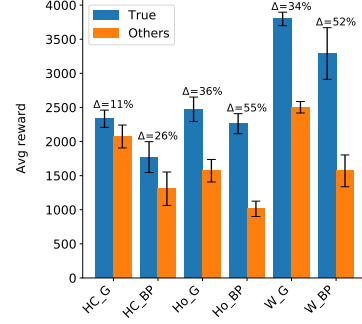


Figure C.1: Performance with the true policy vs other policies. Percent gap (Δ) indicates task diversity. Body parts (BP) domains are more diverse than gravity (G) domains, and Walker-2D (W) and Hopper (Ho) domains are more varied than HalfCheetah (HC) domains.

Table D.1: Results with different versions of EWC. EWC regularization with σ shared across tasks (boldfaced) was the most consistent, so we chose this for our experiments in the main paper.

Domain	Algo	Start	Tune	Final
HC_G	EWC 1, 1	−1245	−2917	−3.97e4
	EWC 1, 2	1796	2409	2603
	EWC 1, 3	1666	2225	2254
	EWC 2, 1	−778	1384	1797
	EWC 2, 2	−762	1565	2238
	EWC 2, 3	−6.58e5	−7e5	−1.05e7
HC_BP	EWC 1, 1	1029	1748	1522
	EWC 1, 2	1132	1769	1588
	EWC 1, 3	1077	1716	1571
	EWC 2, 1	−892	1308	1521
	EWC 2, 2	−1.79e5	−2.16e5	−1.53e6
	EWC 2, 3	−1.1e6	−1.01e6	−5.23e6
Ho_G	EWC 1, 1	1301	2252	1522
	EWC 1, 2	1339	2322	1836
	EWC 1, 3	1434	2488	1732
	EWC 2, 1	872	2616	2089
	EWC 2, 2	930	2582	1900
	EWC 2, 3	939	2520	2029
Ho_BP	EWC 1, 1	613	1508	793
	EWC 1, 2	385	920	43
	EWC 1, 3	424	936	31
	EWC 2, 1	615	2142	1011
	EWC 2, 2	620	2119	1120
	EWC 2, 3	613	2138	928
W_G	EWC 1, 1	1293	2052	303
	EWC 1, 2	−2132	−2181	NaN
	EWC 1, 3	2192	3901	2325
	EWC 2, 1	−2269	−1915	−2490
	EWC 2, 2	−3.12e4	−3.23e4	−1.15e5
	EWC 2, 3	−8.98e4	−9.65e4	−1.59e5
W_BP	EWC 1, 1	1237	3055	1382
	EWC 1, 2	1148	2800	1306
	EWC 1, 3	744	2000	−128
	EWC 2, 1	NaN	NaN	NaN
	EWC 2, 2	1027	3687	1416
	EWC 2, 3	NaN	NaN	NaN